Life Sciences 237 (2019) 116893

Contents lists available at ScienceDirect

Life Sciences

journal homepage: www.elsevier.com/locate/lifescie

Physcion 8-O-β-glucopyranoside induced ferroptosis via regulating miR-103a-3p/GLS2 axis in gastric cancer

Ying Niu, Jinping Zhang, Yalin Tong, Jiansheng Li, Bingrong Liu*

Department of Gastroenterology, the First Affiliated Hospital of Zhengzhou University, Zhengzhou, China

ARTICLE INFO

Keywords:
Gastric cancer
Physcion 8-O-β-glucopyranoside
Ferroptosis
Malignant biological behavior

ABSTRACT

Aim: Gastric cancer (GC) is a common human malignancy tumor of digestive tract in worldwide. Physcion 8-O-β-glucopyranoside (PG) exhibits anti-tumor effects in various cancer cells. This study aimed to explore the biological behavior effects of PG on GC cells, and determine its underlying mechanism.

Material and methods: The effect of PG treatment on the ferroptotic GC cell death was detected by ROS level, intracellular Fe^{2+} level and malondialdehyde (MDA) generation *in vitro*. The mRNA expression was detected by RT-qPCR. The interaction between miR-103a-3p and glutaminase 2 (GLS2) were verified by dual-luciferase reporter gene assay. Cell proliferation, invasion and migration were examined by CCK-8 and Transwell assay. Western blot was used to examine the expression of GLS2, SLC1A5 and epithelial-mesenchymal transition (EMT) related proteins. We also evaluated the influence of PG on the tumor growth and metastasis *in vivo*.

Results: PG-induced ferroptosis in GC cells through upregulating ROS level, intracellular Fe^{2+} level and MDA generation. Besides, PG also significantly enhanced the protein level of GLS2, which was an important transporter of glutamine to glutamate. Importantly, miR-103a-3p directly interacted with GLS2 and suppressed its expression. Mechanistically, PG treatment significantly promoted ferroptosis and anti-tumorigenesis by down-regulating inhibitory effect of miR-103a-3p on GLS2 expression.

Conclusion: Our studies confirmed that PG exerts pro-ferroptosis and anti-tumor effects *in vitro* and *in vivo* through regulating miR-103a-3p/GLS2 axis, thereby highlighting its therapeutic potential in GC.

1. Introduction

Gastric cancer (GC) is a serious malignant tumor threatening the survival and health of all human beings, and Asia is one of the high-incidence areas [14]. In China, the incidence number of GC ranks first in Asia and the incidence and mortality rate are among the top three in all malignant tumors [10]. Due to the early symptoms are not clear and lack of standardized physical examination, the majority of patients with GC already have metastasis, which lead to poor prognosis. Therefore, to explore the molecular mechanism of metastasis and search for effective therapeutic agents/drugs against GC may provide a new point for the prediction, diagnosis and treatment of GC metastasis.

Chinese medicine in the treatment of malignant tumor has a significant advantage [1,16], a large number of basic and clinical research at home and abroad have confirmed that traditional Chinese medicine through multi-channel, multi-target, multi-link plays a role, with comprehensive onset characteristics, so as to play a preventive and treatment of tumor efficacy [27]. Of note, the natural plant and its active ingredients of antitumor activity has been initially recognized by the international medical profession [7]. Physcion 8-O-β-glucopyranoside (PG) is one of the chemical components contained in Rumex japonicus Houtt, and current studies have demonstrated the PG has antitumor effects in multiple solid tumor [36]. For example, PG-induced apoptosis and inhibited proliferation, invasion and migration of cancer cells, including glioblastoma [18], hepatocellular carcinoma [30] and cell renal cell carcinoma (Wang et al., 2018a), etc. However, the anti-tumor effects of PG on the growth and metastasis of GC is still unknown.

Ferroptosis is a newly-established form of regulated cell death, which is coined after the requirement for free ferrous iron [33]. Biochemically, the process of ferroptosis is characterized by accumulation of lipid peroxidation products and lethal reactive oxygen species (ROS) derived from iron metabolism. Of note, ferroptosis plays an important role involved in regulating the progression of multiple tumors, including breast cancer [37], colon cancer [21], liver cancer [41], etc. In addition, previous studies have showed that natural active components alleviated multidrug resistance of cancer and inhibit the progression of multiple tumors through inducing ferroptosis [12,17]. For example, artemisinin compounds exhibit antitumor effects in multiple tumor cells

* Corresponding author. Jianshe East Road 1, Zhengzhou, 450052, China.
E-mail address: bingrongliuzzah@163.com (B. Liu).

https://doi.org/10.1016/j.lfs.2019.116893
Received 2 August 2019; Received in revised form 10 September 2019; Accepted 19 September 2019
Available online 10 October 2019
0024-3205/

via inhibiting GPX4 expression to induce ferroptosis [5]. Furthermore, accumulating evidence confirmed that microRNA (miRNA) targets downstream gene to induced ferroptosis in cancer cells [35,40]. These results indicated that a tumor suppressive function of ferroptosis in malignant tumor, but its underlying mechanism was needed to be elucidated further. This study was aimed to determine the role of PG in GC progression through mediating ferroptosis and its potential anti-tumorigeneses mechanism.

2. Materials and methods

2.1. Cell culture

GC cell lines (MGC-803 and MKN-45) were obtained from the Chinese Academy of Sciences Cell Bank (Shanghai, China). Both cells were maintained in Dulbecco's modified Eagle medium (Gibco BRL, USA) containing 10% fetal bovine serum (Hyclone, Logan, USA) at 37 °C in a humidified atmosphere containing 95% air and 5% CO_2.

2.2. Cell transfection

The MGC-803 and MKN-45 cells were seeded in six-well plates with optimum density and then incubated overnight. miR-103a-3p mimics/inhibitor, pcDNA-GLS2, GLS2 siRNA and control vector were transfected into both GC cells with Lipofectamine 3000 reagent (Invitrogen Life Technologies, USA) and Opti-MEM medium (Invitrogen Life Technologies, USA) in the light of the specification. The miR-103a-3p mimics/inhibitor, pcDNA-GLS2, GLS2 siRNA and control vector were bought from Tolo Biotech (Shanghai, China).

2.3. RT-qPCR

Total RNA was extracted from the cells using Trizol reagent (Takara, Japan). Reverse transcription was performed using the PrimeScriptTM RT reagent Kit with gDNA Eraser (Takara, Japan) according to the manufacturer's protocol. RT-qPCR was performed using the SYBR Premix Ex Taq (Takara, Japan) under standard conditions according to the manufacturer's instruction. RT-qPCR was conducted with CFX96 Real-Time PCR Detection System (Bio-Rad, USA). The sequence of quantitative PCR primers of miR103a-3p and U6 were purchased from Shanghai GenePharma Co., Ltd (Shanghai, China), U6 as the internal control. The $2^{-\Delta\Delta Ct}$ methods were applied to calculate the relative expression levels of total mRNA. The experiment for each group was repeated three times.

2.4. CCK-8 assay

Cell counting kit-8 (CCK-8, Sigma, Japan) was used to detect the proliferation of MGC-803 and MKN-45 cells. Cells were seeded in 96-well plates at a density of 1×10^4 cells per well and cultured with 5% CO_2 at 37 °C an incubator for 2 h to allow cells adhere. A total of 10 μL CCK-8 solution was added to each well and mixed, and cells were incubated for a further 2 h. A dual-wavelength microplate reader was used to measure proliferation at 450 nm (Beckman Coulter, USA). Each experiment was set up with three parallel repeats.

2.5. Transwell invasion and migration assay

Matrigel (BD Biosciences, USA) (only for invasion assay) was coated the upper surface of polycarbonate filters. Paced the 1×10^4 (for migration assay) or 5×10^4 (for invasion assay) cells on the surface of the Transwell upper chamber. After 24 h, the migration and invasive cells were fixed with 4% PFA (paraformaldehyde) and rinsed three times with PBS, then stained with 0.1% crystal violet for 10 min and rinsed three times with PBS. Random selection 5 fields of vision for cell count, observation and photography.

2.6. Western blot

Total protein was extracted for Western blot analysis. The PVDF (polyvinylidene fluoride) was incubated overnight at 4 °C with the primary antibodies against SLC1A5 (1:1000, ab58690, Abcam, UK), GLS2 (1:1000, ab113509, Abcam, UK), E-cadherin (1:1000, ab1416, Abcam, UK), N-cadherin (1:1000, ab18203, Abcam, UK), Vimentin (1:1000, ab8978, Abcam, UK), and subsequently incubated with a horseradish peroxidase-coupled secondary antibody (1:4000, Abcam, UK). β-actin was the internal reference. Signals were detected with chemiluminescence using an ECL kit (Bio-Rad, USA).

2.7. Dual-luciferase reporter gene assay

The cells were seeded in 24-well plates at a density of 60%. according to the manufacturer's instructions, the reporter construct containing GLS2 wild-type or mutant 3′UTR was co-transfected into cells with miR-103a-3p using Lipofectamine 3000 reagent. After 48 h, the cells were collected and tested for luciferase by dual-luciferase assay system (Promega, USA).

2.8. Nude mice model

Female BALB/c nude mice (4–5 weeks old) were purchased from SLAC Laboratory Animal Co., Ltd. (Shanghai, China). The model was approved by the Ethical Committee of First Affiliated Hospital of Zhengzhou University. MGC-803 cells (1×10^6) were suspended in serum-free DMEM medium and then inoculated in (10 mice in each group) at 6–7 weeks old. After 21 days of adaptive feeding, a total of 30 mice were randomly divided into three groups: control and PG at the dose of 30 mg/kg/d or 50 mg/kg/d group. Mice in PG group were injected intraperitoneally with 30 mg/kg/d or 50 mg/kg/d PG (Beijing Sollarbio Science & Technology, China). Mice in control group were injected with 0.9% sodium chloride plus 1% DMSO. Tumor growth was recorded every three days by measuring tumor length and width. After 4 weeks incubation, the mice were killed and the mice tumor tissues to be collected for further evaluated. And hematoxylin and eosin (H&E) and immunohistochemistry staining was applied to observe the histomorphology and examine the expression of Ki-67, E-cadherin and Vimentin according to the previous studies [9].

2.9. Determination of ROS level, MDA generation and intracellular Fe^{2+} level

The expression of expression level of ROS and Fe^{2+}, and MDA generation in cells or tissues were determined by using DCF ROS Assay Kit (ab238535, Abcam, UK), Iron Assay Kit (ab83366, Abcam, UK) and Lipid peroxidative Assay Kit (ab118970, Abcam, UK) under standard conditions according to the manufacturer's instructions. The experiment for each group was repeated three times.

2.10. Statistical analysis

The experimental data and image preprocessing were respectively analyzed by SPSS 20.0 statistical software (IBM, USA) and GraphPad Prism8.0 software (La Jolla, USA). Besides, student's t-test was used to analyze the significant difference between the two-independent group, and the differences between multiple groups were compared by one-way ANOVA. Moreover, $P < 0.05$ was identified as statistically significant.

3. Results

3.1. PG induced ferroptosis in gastric cancer cells

Previous studies confirmed that PG exhibits antitumor effects in

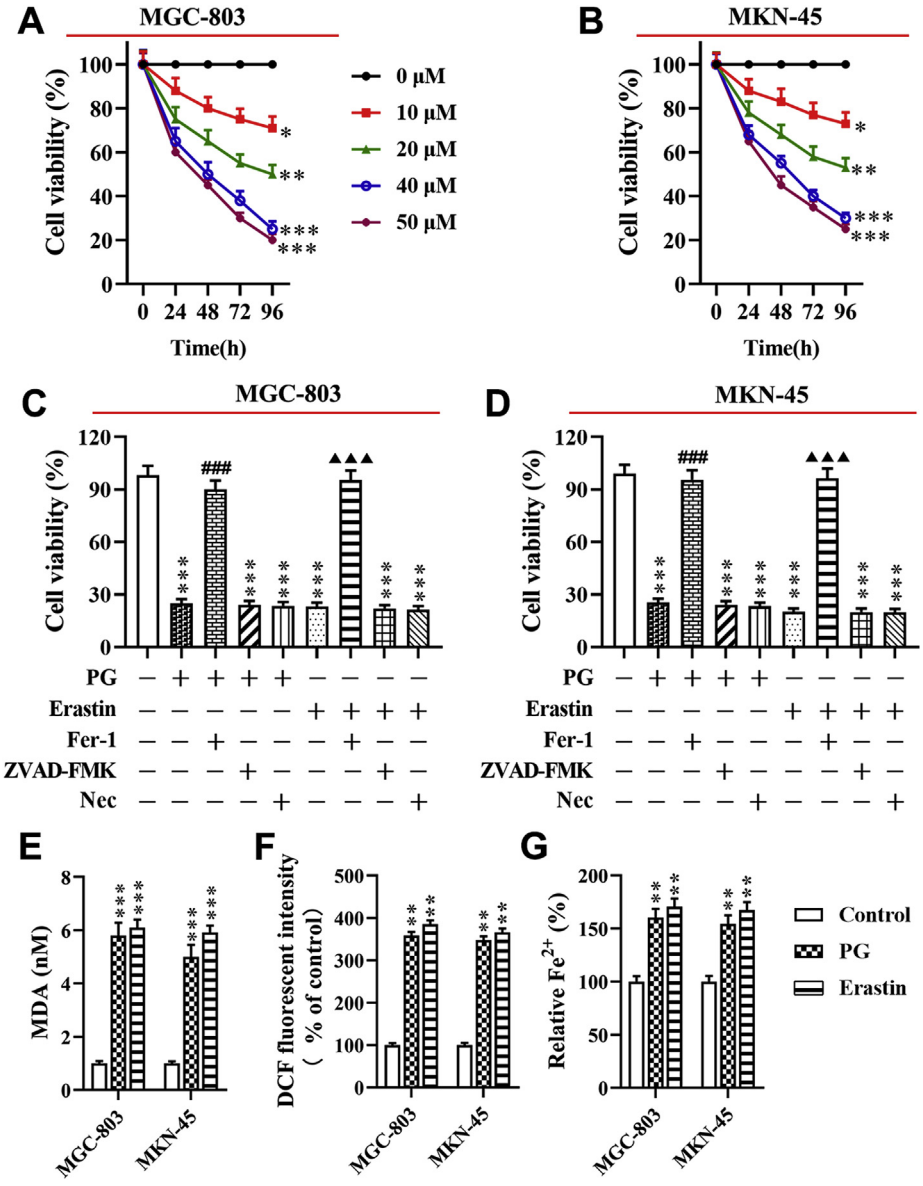

Fig. 1. PG induced ferroptosis in gastric cancer cells A and B: CCK-8 was used to detect cell viability in both MGC-803 and MKN-45 cells treated with different concentration of PG for 24 h; C and D: CCK-8 was applied to evaluate proliferation ability of both MGC-803 and MKN-45 cells treated with PG plus cell death inducer erastin or inhibitor (Fer-1, ZVAD-FMK, and Nec); E: The level of MDA was measured by lipid peroxidative assay kit; F: The lipid ROS levels was determined by lipid ROS assay; G: The intracellular Fe^{2+} was detected by iron assay kit. *P < 0.05, **P < 0.01, ***P < 0.001, compared with control group; ###P < 0.001, compared with PG treatment group; ▲▲▲P < 0.001, compared with erastin treatment group.

tumor cells through inducing cell apoptosis [18]. In this study, CCK-8 assay was used to evaluate the proliferation of MGC-803 and MKN-45 cells treated with PG at the dose of 10, 20, 40 and 50 μM for 24 h. The result showed that PG significantly inhibited both cell viability in a dose-dependent manner (Fig. 1A, B). However, there was no significant difference in the concentration of PG between 40 μM and 50 μM. Moreover, to further prove whether the Ferroptosis caused this result in both MGC-803 and MKN-45 cells, we treated both cell lines with several cell death inhibitors. As shown in Fig. 1C and D, treatment with PG or ferroptosis inducer erastin significantly decreased the proliferation of MGC-803 and MKN-45 cells compared with the control group (all $P < 0.001$). Besides, pre-treating both cells with ferroptosis inhibitor Ferrostatin-1 (Fer-1) abolished PG-induced ferroptosis ($P < 0.001$, Fig. 1C, D), but not apoptotic inhibitor ZVAD-FMK and necroptotic inhibitor Necro-sulfonamide (Nec). Furthermore, we assessed two main events in the process of ferroptosis, including lipid peroxidative and iron accumulation. The results showed that PG or erastin treatment notably increased the levels of ROS and MDA generation ($P < 0.01$, $P < 0.001$, Fig. 1E, F), as well as enhanced intracellular Fe^{2+} level in both MGC-803 and MKN-45 cells (all $P < 0.01$, Fig. 1G). Taken together, PG exhibits anti-proliferation effects in MGC-803 and MKN-45 cells through inducing ferroptosis.

3.2. Inhibition of Glutamine uptake was a required for PG-induced ferroptosis in MGC-803 and MKN-45 cells

Increasing evidence confirmed that glutamine metabolism plays an important role involved in regulating ferroptosis induced by lipid peroxidative in cancer cells [3], and its detail regulation process was shown in Fig. 2A. In this study, both MGC-803 and MKN-45 cells treated with key regulatory gene inhibitors (GPNA and compound 968 (968)) of glutamine metabolism in the process of ferroptosis, and their viability were determined by CCK-8. As shown in Fig. 2B and C, PG significantly suppressed the viability of MGC-803 and MKN-45 cells (all $P < 0.001$), while pre-treated with GPNA or 968 markedly attenuated PG-induced cell death in both cell lines (all $P < 0.001$). To further validate this hypothesis, our finding showed that GPNA and 968 attenuated PG-induced ferroptosis by decreasing intracellular Fe^{2+} levels (all $P < 0.01$, Fig. 2C, D), MDA generation (all $P < 0.001$, Fig. 2F, G) and ROS level (all $P < 0.001$, Fig. 2H, I). Furthermore, we also analyzed the protein levels of GLS2 and SLC1A5 in MGC-803 and MKN-45 cells, and found that PG significantly enhanced the expression of GLS2 (both $P < 0.001$, Fig. 2J-M), but did not affect SLC1A5 expression. Taken together, PG-induced ferroptosis in the MGC-803 and MKN-45 cells via regulating GLS2-mediated glutamine metabolism.

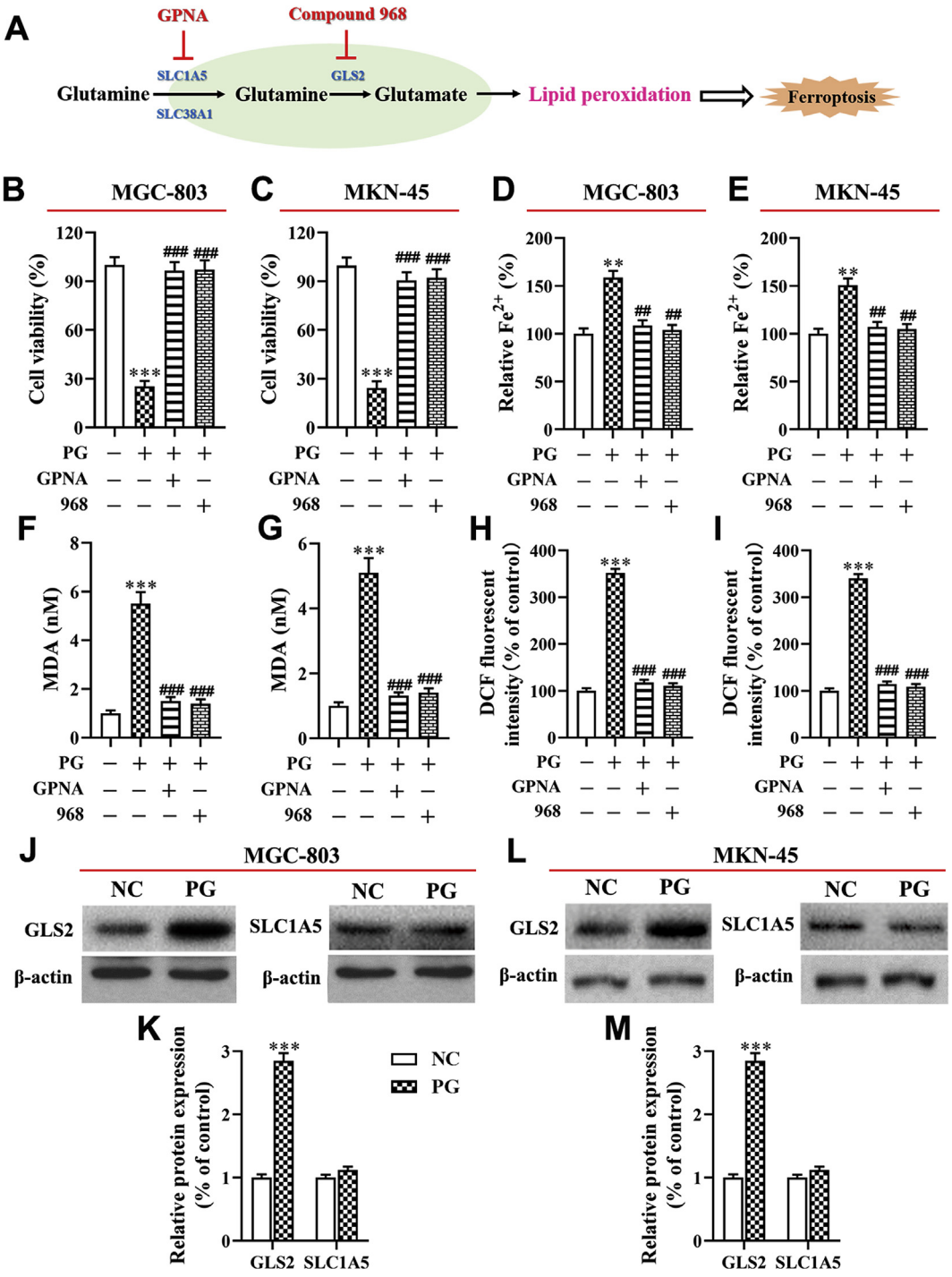

Fig. 2. Inhibition of Glutamine uptake was a required for PG-induced ferroptosis in MGC-803 and MKN-45 cells. A: The schematic representation of glutamine metabolic in ferrpoptotic gastric cancer cell death; B and C: CCK-8 was used to assess the effect of glutamine transporter inhibitor (GPNA) and GLS2 inhibitor (compound 968) on proliferation ability of both MGC-803 and MKN-45 cells; D and E: The intracellular Fe^{2+} was detected by iron assay kit; F and G: The level of MDA was measured by lipid peroxidative assay kit; H and I: The lipid ROS levels was determined by lipid ROS assay; J–M: Western blot was applied to detect the levels of GLS2 protein in both gastric cancer cells. $^{**}P < 0.01$, $^{***}P < 0.001$, compared with NC group; $^{\#\#}P < 0.01$, $^{\#\#\#}P < 0.001$, compared with PG treatment group.

3.3. PG-induced ferroptosis by upregulating GLS2 expression

GLS2 plays an important role in the transformation of glutamine to glutamate, and knockdown of GLS2 could block ferroptosis in cancer cells [15]. We further to evaluate the role of GLS2 involved in PG-induced ferroptosis by regulating glutamine metabolism. Primally, both MGC-803 and MKN-45 cells transfected with GLS2 siRNA, and its transfection efficiency was detected by Western blot (both $P < 0.001$, Fig. 3A–C). Moreover, knockdown of GLS2 significantly repressed the inhibitor effect of PG on cell viability in both MGC-803 and MKN-45 cells (all $P < 0.01$, Fig. 3D, E). Furthermore, knockdown of GLS2 notably alleviated the PG-induced ROS level (both $P < 0.001$, Fig. 3F), MDA production (both $P < 0.001$, Fig. 3G), and intracellular Fe^{2+} levels (both $P < 0.01$, Fig. 3H). Collectively, PG-induced ferroptosis through upregulating GLS2 in both MGC-803 and MKN-45 cells.

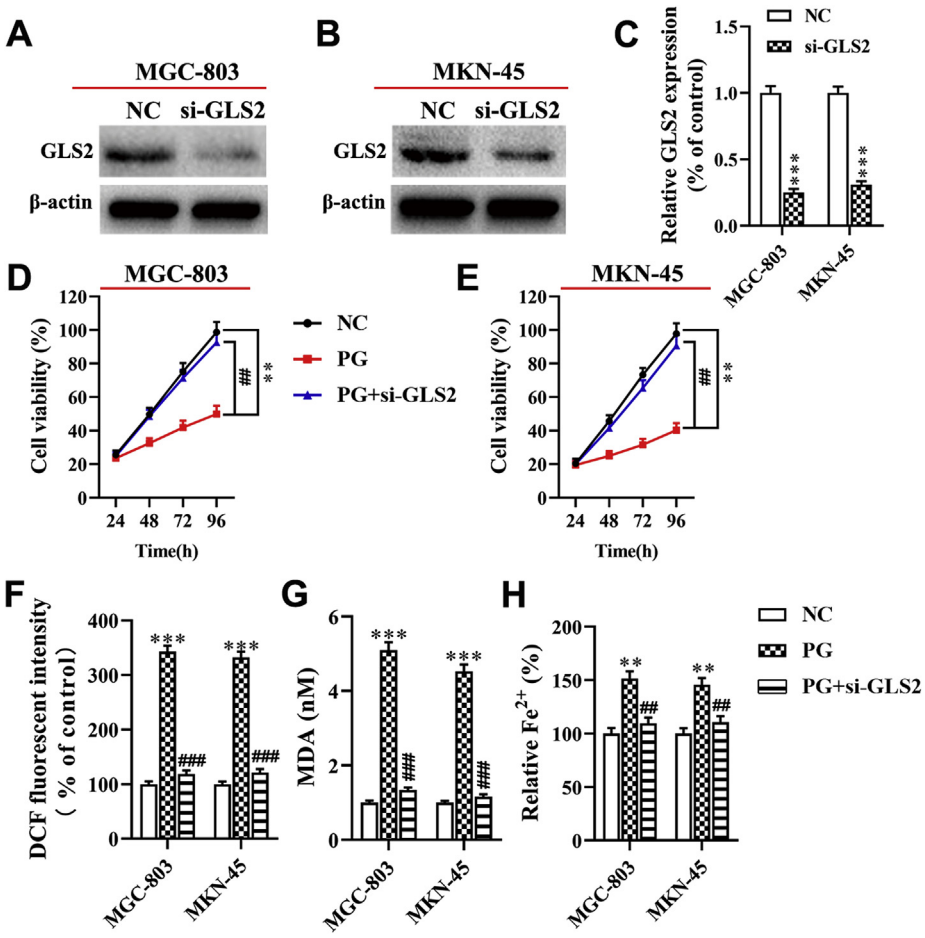

Fig. 3. PG-induced ferroptosis by upregulating GLS2 expression A–C: Western blot was applied to measure the expression of GLS2 protein; D and E: CCK-8 was used to detect the cell viability in both MGC-803 and MKN-45 cells; F: The lipid ROS levels was determined by lipid ROS assay; G: The level of MDA was measured by lipid peroxidative assay kit; H: The intracellular Fe^{2+} was detected by iron assay kit. **P < 0.01, ***P < 0.001, compared with NC group; ##P < 0.01, ###P < 0.001, compared with PG treatment group.

3.4. miR-103a-3p directly targeted GLS2 in gastric cancer cells

To further understand the mechanism underlying the effect of GLS2 on PG-induced ferroptosis, we discovered that miR-103a-3p may targeted GLS2 directly from the starBase database (http://starbase.sysu.edu.cn/) (Fig. 4A). To further confirm that miR-103a-3p was specifically binding to the 3′UTR region of GLS2 mRNA to regulate the expression of GLS2 by dual-luciferase reporter gene assay. The results showed that luciferase activity in GLS2-WT + miR-103a-3p mimics group was lower than GLS2-WT + miR-NC group (P < 0.01, Fig. 4B), but there was no significant difference exist between miR-103a-3p mimics or NC were transferred in the GLS2-MUT group (P > 0.05).

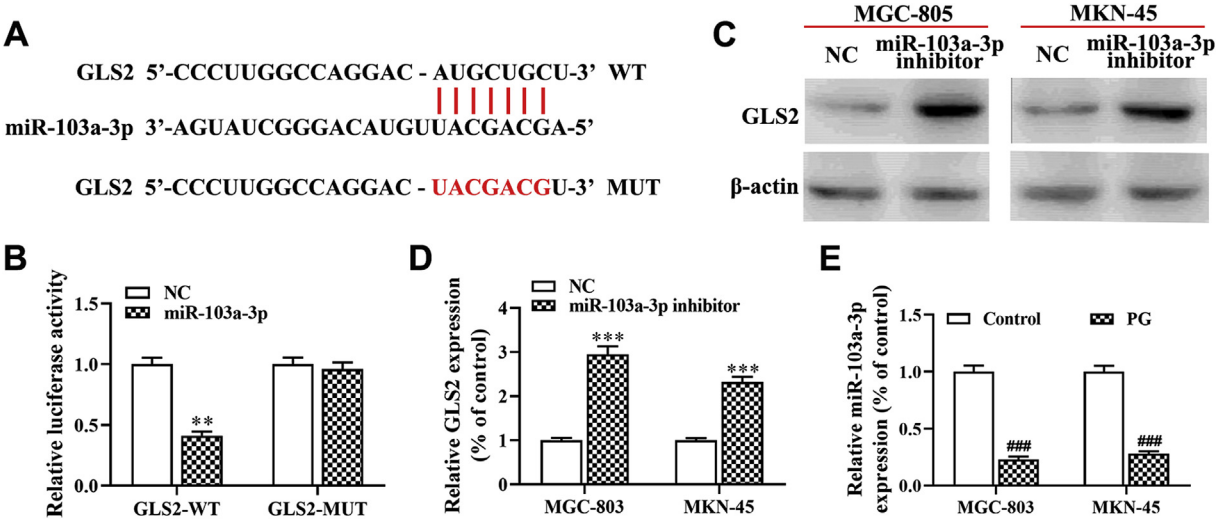

Fig. 4. The regulatory relationship between miR-103a-3p and GLS2. A: The bioinformatics analysis result showed that miR-103a-3p had a binding site with GLS2; B: Dual luciferase reporter gene assay was used to verify the target relationship between miR-103a-3p and GLS2; C and D: The expression of GLS2 protein was detected by Western blot; E: The expression of miR-103a-3p was determined by RT-qPCR. **P < 0.01, ***P < 0.001, compared with NC group; ###P < 0.001, compared with control group.

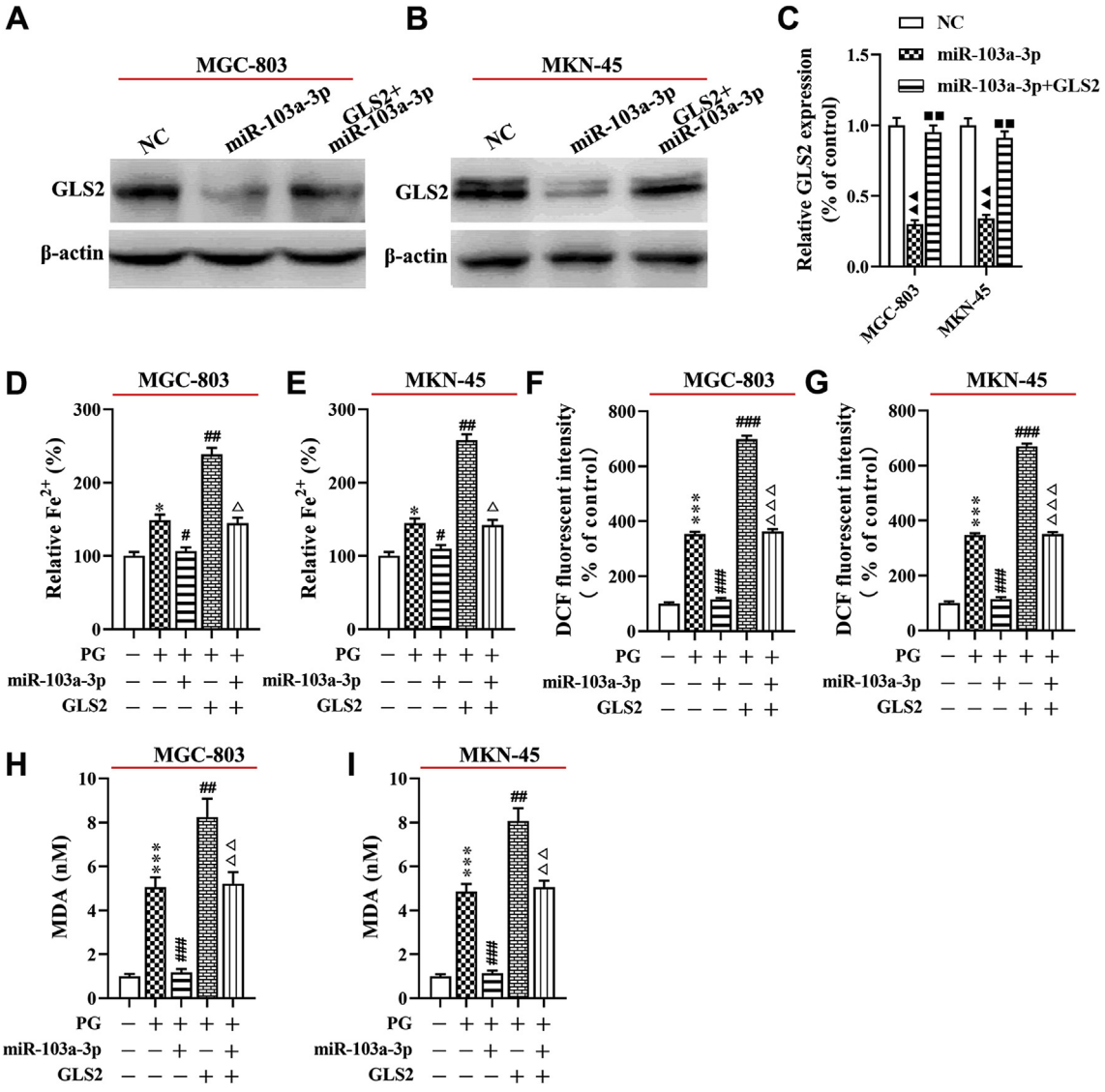

Fig. 5. PG-induced ferroptosis via regulating miR-103a-3p/GLS2 axis A–C: The expression of GLS2 protein was detected by Western blot; D and E: The intracellular Fe^{2+} was detected by iron assay kit; F and G: The lipid ROS levels was determined by lipid ROS assay; H and I: The level of MDA was measured by lipid peroxidative assay kit. ▲▲P < 0.01, compared with NC group; ■■P < 0.01, compared with miR-103-3p group; *P < 0.05, ***P < 0.001, compared with control group; #P < 0.05, ##P < 0.01, ###P < 0.001, compared with PG group; △P < 0.05, △△P < 0.01, △△△P < 0.001, compared with PG + miR-103a-3p + GLS2 group.

Meanwhile, we used Western blot to test the expression level of GLS2 when miR-103a-3p inhibitor was transfected into MGC-803 and MKN-45 cells. The analysis results pointed out that silencing of miR-103a-3p significantly increased the expression of GLS2 protein (both P < 0.001, Fig. 4C, D). Furthermore, PG-treated notably decreased the expression of miR-103a-3p in both MGC-803 and MKN-45 cells compared with the control group (both P < 0.001, Fig. 4E). Taken together, these results suggested that GLS2 was the direct target of miR-103a-3p which was negatively regulated GLS2 expression.

3.5. PG-induced ferroptosis via regulating miR-103a-3p/GLS2 axis

To further determine the role of miR-103a-3p/GLS2 axis in regulating PG-induced ferroptosis in both MGC-803 and MKN-45 cells. Western blot results showed that the expression of GLS2 protein was significantly decreased in both MGC-803 and MKN-45 cells when transfected with miR-103-3p mimics (both P < 0.01, Fig. 5A–C), while co-transfected miR-103a-p mimics and pcDNA-GLS2 alleviated this effect (both P < 0.01). Moreover, overexpression of miR-103a-3p significantly downregulated the promotion effect of PG on the intracellular Fe^{2+} level (both P < 0.05, Fig. 5D, E), ROS level (both P < 0.01, Fig. 5F, G) and MDA (both P < 0.001, Fig. 5H, I) in both MGC-803 and MKN-45 cells. However, the inhibitory effect of miR-103a-3p on ferroptosis of both MGC-803 and MKN-45 cells were reversed by co-transfecting with pcDNA-GLS2 (Fig. 5D–I). These results suggested that PG promoted ferroptosis in both MGC-803 and MKN-45 cells through downregulating inhibitory effect of miR-103a-3p on GLS2 expression.

3.6. PG suppresses proliferation and metastasis of gastric cancer cells via regulating miR-103a-3p/GLS2 axis

To further explore the anti-tumor effect of PG on gastric cancer through miR-103a-3p/GLS2 axis *in vitro*. Our studies revealed that overexpression of miR-103a-3p significantly downregulated the inhibitory effect of PG-treated on the proliferation, invasion and migration of MGC-803 and MKN-45 cells (P < 0.01, P < 0.001, Fig. 6A–H). However, the upregulation effect of miR-103a-3p on the malignant biological behavior of MGC-803 and MKN-45 cells were reversed by co-transfecting with pcDNA-GLS2 (all P < 0.01, Fig. 6A–H). Moreover,

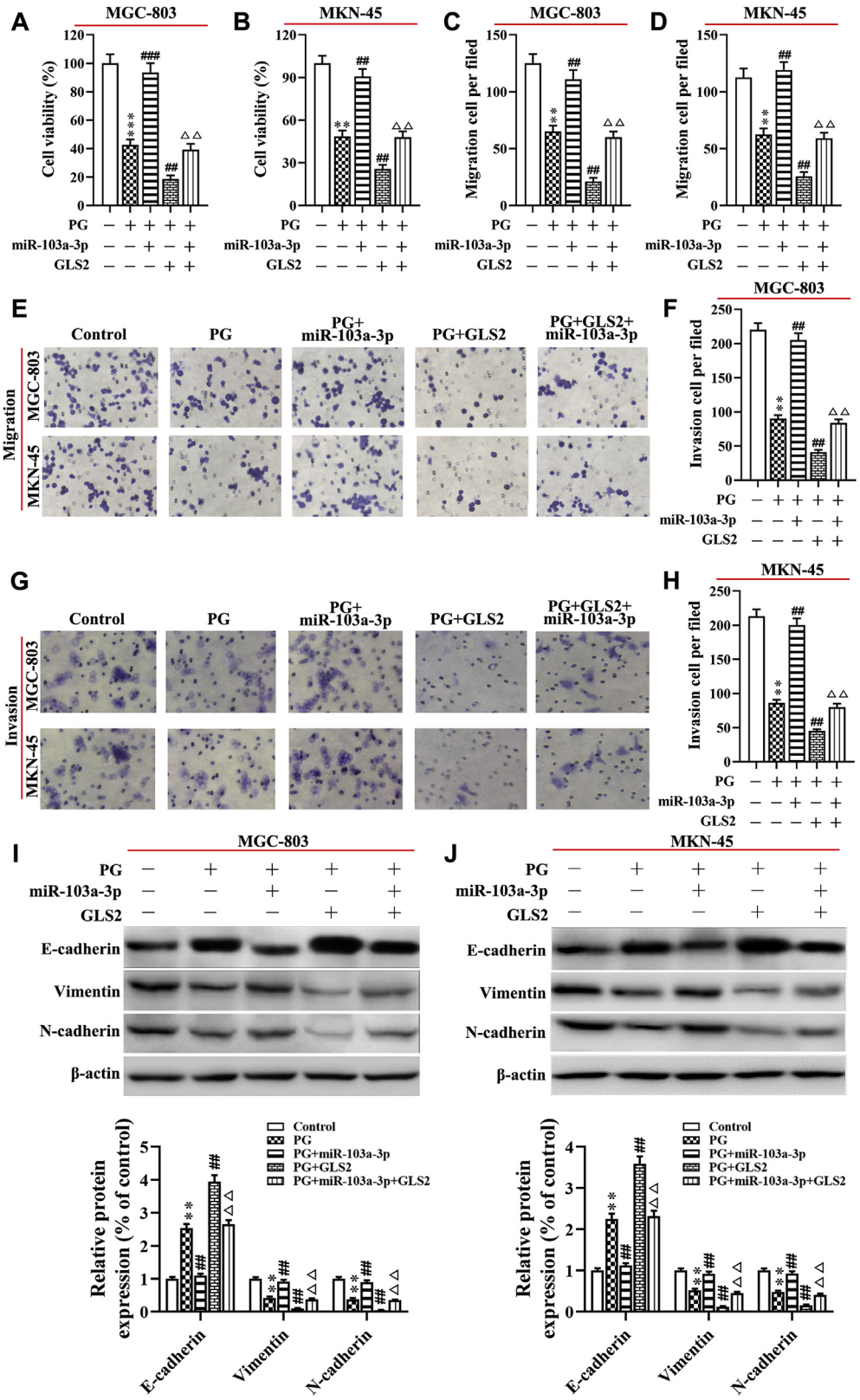

Fig. 6. PG suppresses proliferation and metastasis of gastric cancer cells via regulating miR-103a-3p/GLS2 axis A and B: The proliferation of both MGC-803 and MKN-45 cells were detected by CCK-8 assay; C–H: Transwell was used to evaluate the migration and invasion ability of MGC-803 and MKN-45 cells; I–L: Western blot was applied to detect the expression of EMT related proteins in both MGC-803 and MKN-45 cells. $^{**}P < 0.01$, $^{***}P < 0.001$, compared with control group; $^{\#\#}P < 0.01$, $^{\#\#\#}P < 0.001$, compared with PG treated group; $^{\triangle\triangle}P < 0.01$, compared with PG + miR-103a-3p + GLS2 group.

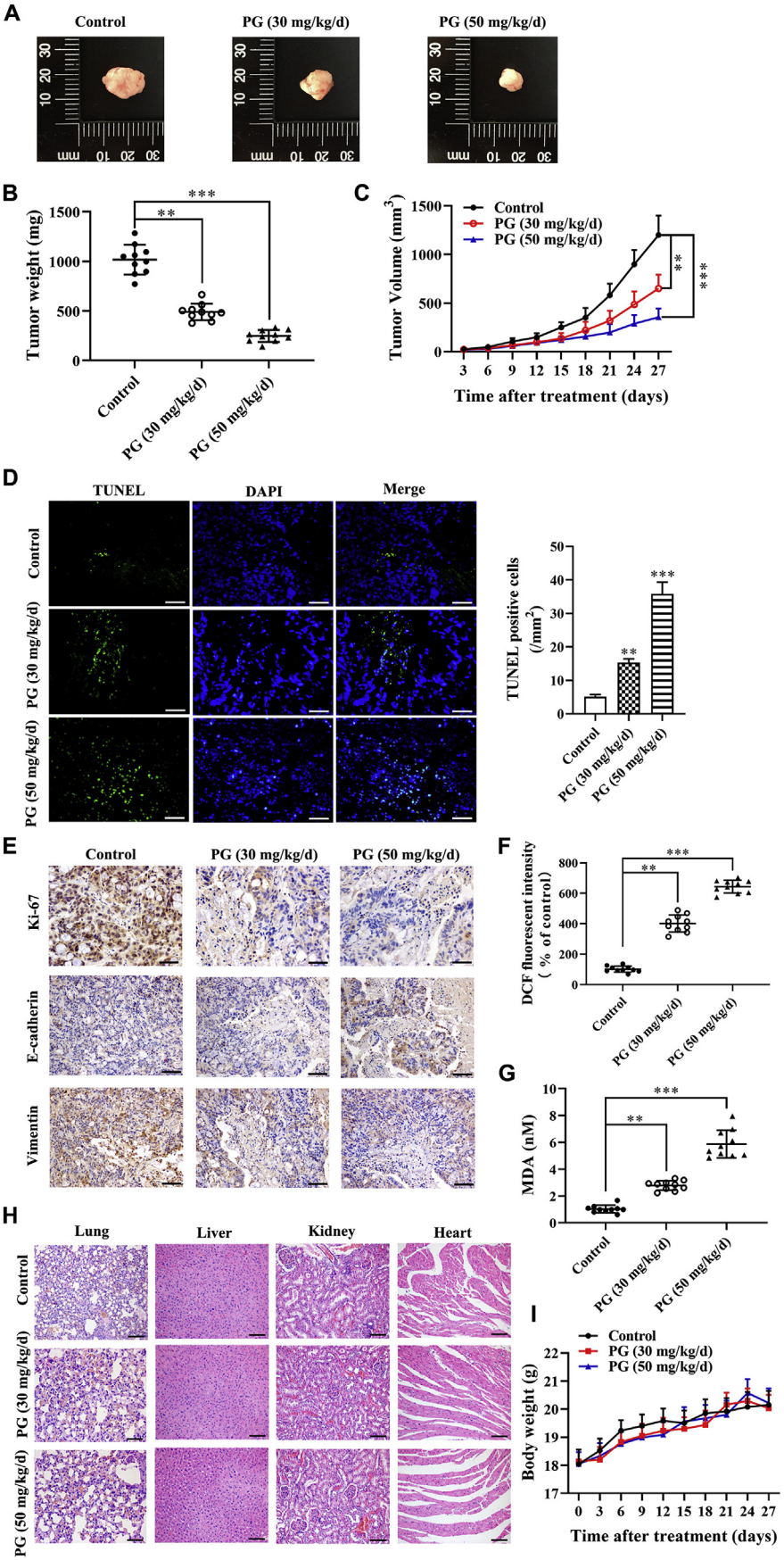

Fig. 7. PG suppresses growth and metastasis of gastric cancer. A: The tumor size was obtained from nude mice; B: The tumor weight was measured; C: The tumor volume curve of nude mice treated with BAN (30 mg/kg/d) or control was analyzed; D: The apoptotic cells was detected by TUNEL staining; E: The expression of Ki-67, E-cadherin and Vimentin were detected in tumor tissues by immunohistochemistry; F: The lipid ROS levels was determined by lipid ROS assay; G: The level of MDA was measured by lipid peroxidative assay kit; H: HE staining was applied to evaluate the changes in the lung, heart, kidney and liver tissues; I: The body weight of nude mice were measured. **P < 0.01, ***P < 0.001, compared with control group.

Western blot showed that upregulation of miR-103a-3p significantly decreased PG-induced EMT of MGC-803 and MKN-45 cells (all $P < 0.01$, Fig. 6I, J). However, no significant difference between only PG-treated group and miR-103a-3p + GLS2 + PG group (Fig. 6). Taken together, these results confirmed that PG administration suppressed proliferation and metastasis of MGC-803 and MKN-45 cells through mediating miR-103a-3p/GLS2 axis.

3.7. PG suppresses growth and metastasis of tumor in vivo

The role of PG was also evaluated in a xenograft model of gastric cancer. As shown in Fig. 7A–C, both 30 and 50 mg/kg/day doses of PG significantly suppressed tumor growth in terms of weight and volume ($P < 0.01$, $P < 0.001$). Moreover, PG markedly increased the percentage of TUNEL positive apoptotic cells in the tumors ($P < 0.01$, $P < 0.001$, Fig. 7D, E). Besides, immunohistochemistry results showed that PG also decreased the expression of vimentin and Ki-67 in the tumors tissues (Fig. 7E), but increased the expression of E-cadherin, indicating a potent anti-proliferative and anti-metastasis effect *in vivo*. As expected, PG significantly enhanced the ROS level and MDA production in tumor tissues compared with the untreated group ($P < 0.01$, $P < 0.001$, Fig. 7F, G). Furthermore, to evaluate the safety of PG, the body weight of the mice, pathological changes in the lung, liver, kidney and heart tissues were detected. PG treatment did not cause any acute injury to the major organs (Fig. 7H), nor did it adversely affect the body weight (Fig. 7I). Taken together, PG exhibits anti-tumor effect in gastric cancer through inducing ferroptosis.

4. Discussion

GC, the fourth most commonly cancer in the world, is a major public health problem that needs to be solved on a global scale. In this study, we discussed the molecular mechanism of PG inhibits malignant biological behavior of GC cells through regulating ferroptosis. PG-treated significantly induced ferroptosis and inhibited migration and invasion of MGC-803 and MKN-45 cells, but enhanced the expression of GLS2 protein. Mechanically, overexpression of miR-o103a-3p targets GLS2 to alleviate PG-induced ferroptosis and antitumorigenic *in vitro* and *in vivo*. Hence, PG significantly trigged the GC cells ferroptosis and suppressed biological behavior by downregulating the inhibitory effect of miR-103a-3p on GLS2 expression and provided a new tool for target treatment of GC patients.

In recent years, increasing evidence suggest that ferroptosis plays an important regulatory role in radiotherapy, chemotherapy and development and progression of multiple malignant tumors. For example, activation of ferroptosis was attenuated cancer cells-acquired drug resistance and immune evasion [8]. Sui et al. found that ferroptosis inducer RSL3 decreased the progression of colorectal cancer through GPX4 inactivation and ROS generation [26]. In addition, GLS2 was a master transporter that regulated glutamine converted to glutaminase in mitochondria [4,20]. Interestingly, glutaminolysis pathway was a key regulator of cell growth, apoptosis, ferroptosis, autophagy [23,28]. Luo et al. showed that inhibition of GLS2 was repressed ferroptosis induced by lipid peroxidative in melanoma [19]. Meanwhile, GLS2, which is a target gene of p53, was exerted antitumor effect in cancer cells by inducing ferroptosis [13]. Furthermore, GLS2-mediated glutamine metabolism and its expression were negative correlated with malignant and growth of tumor [22]. In the present study, our finding revealed that upregulation of GLS2 inhibited proliferation and metastasis of GC cells, and promoted ROS level and MDA generation, which was induced by PG treatment.

Accumulating evidence has reported that PG plays important role in the control of proliferation and metastasis of cancer cells, including melanoma [38], breast cancer [6] and hepatocellular carcinoma [31]. Moreover, PG regulated the progression of malignant tumor by maintaining ATP levels in response to energy stress caused by mitochondrial dysfunction, hypoxia, and shortage of essential metabolic fuel, for example, PG suppressed clear-cell renal cell carcinoma progression by inhibiting glycolysis [32]. Recent studies have confirmed that PG mediates the development of multiple solid tumors by regulating miRNA and its downstream target genes [34]. For instance, Zhang et al. showed that upregulation of miR-124 by PG suppresses proliferation and invasion of melanoma by targeting RLIP76 [38]. In the present study, we demonstrated that PG plays a critical role in the biological behavior of GC cells, and promotes ferroptosis induced by lipid peroxidative. Further studies confirmed that PG inhibits growth and metastasis of GC by downregulating the inhibitory effect of miR-103a-3p on GLS2 expression.

Accumulating evidence confirmed that microRNA (miRNA), as a new type of regulatory factor, plays an important role in tumorigenesis of many malignant tumors including GC, and the role of oncogene or tumor suppressor gene [24,25]. For example, miR-103a-3p, acts a tumor suppressor, was upregulated in gastric cancer, and inhibition of miR-103a-3p was associated with superior outcome [11]. Moreover, miR-103a-3p can be used as a biomarker for early diagnosis of malignant tumors [2,39]. Furthermore, some studies have explored the therapeutic targeting of miRNA in cancer, and miRNAs induced ferroptosis have been confirmed [19,40]. For example, Wang et al. found that miR-6852 targets cystathionine-β-synthase (CBS), a surrogate marker of ferroptosis, to inhibit cell proliferation via inducing ferroptosis in lung cancer [29]. The results of the present study showed that knockdown of miR-103a-3p targets GLS2 to inhibits cell viability and promoted ferroptosis in GC cells, which was induced by PG treatment.

In summary, our results confirmed that PG plays a vital role in the development and progression of GC. Besides, PG dramatically trigger ferroptosis and suppress tumor growth by upregulating GLS2 expression. More importantly, PG exhibits antitumor effects in GC through downregulating inhibitory effect of miR-103a-3p on GLS2 expression. These findings provided a new therapeutic target for the treatment of GC patients.

Author contribution

Bingrong Liu designed the research and provided the fund;
Ying Niu performed the experiments and wrote the paper;
Jinping Zhang and Yalin Tong performed experiments;
Jiansheng Li analyzed the data.

Funding

The work is supported by National Natural Science Foundation of China (81870454).

Declaration of competing interest

None.

References

[1] W. An, H. Lai, Y. Zhang, M. Liu, X. Lin, S. Cao, Apoptotic pathway as the therapeutic target for anticancer traditional Chinese medicines, Front. Pharmacol. 10 (2019) 758.
[2] X. An, H. Quan, J. Lv, L. Meng, C. Wang, Z. Yu, et al., Serum microRNA as potential biomarker to detect breast atypical hyperplasia and early-stage breast cancer, Future Oncol. 14 (2018) 3145–3161.
[3] K. Bartel, H. Pein, B. Popper, S. Schmitt, S. Janaki-Raman, A. Schulze, et al., Connecting lysosomes and mitochondria - a novel role for lipid metabolism in cancer cell death, Cell Commun. Signal. : CCS 17 (2019) 87.
[4] S. Beaudin, J. Welsh, 1,25-Dihydroxyvitamin D regulation of glutamine synthetase and glutamine metabolism in human mammary epithelial cells, Endocrinology 158 (2017) 4174–4188.
[5] G.Q. Chen, F.A. Benthani, J. Wu, D. Liang, Z.X. Bian, X. Jiang, Artemisinin compounds sensitize cancer cells to ferroptosis by regulating iron homeostasis, Cell Death Differ. 21 (2019).
[6] X. Chen, H. Guo, F. Li, D. Fan, Physcion 8-O-beta-glucopyranoside suppresses the

metastasis of breast cancer in vitro and in vivo by modulating DNMT1, Pharmacol. Rep. : PR 69 (2017) 36–44.
[7] J. Du, T. Wang, Y. Li, Y. Zhou, X. Wang, X. Yu, et al., DHA inhibits proliferation and induces ferroptosis of leukemia cells through autophagy dependent degradation of ferritin, Free Radical Biol. Med. 131 (2019) 356–369.
[8] J.P. Friedmann Angeli, D.V. Krysko, M. Conrad, Ferroptosis at the crossroads of cancer-acquired drug resistance and immune evasion, Nat. Rev. Cancer 19 (2019) 405–414.
[9] M. Han, H. Gao, J. Xie, Y.P. Yuan, Q. Yuan, M.Q. Gao, et al., Hispidulin induces ER stress-mediated apoptosis in human hepatocellular carcinoma cells in vitro and in vivo by activating AMPK signaling pathway, Acta Pharmacol. Sin. 40 (2019) 666–676.
[10] N. Hu, Z. Wang, X. Song, L. Wei, B.S. Kim, N.D. Freedman, et al., Genome-wide association study of gastric adenocarcinoma in Asia: a comparison of associations between cardia and non-cardia tumours, Gut 65 (2016) 1611–1618.
[11] X. Hu, J. Miao, M. Zhang, X. Wang, Z. Wang, J. Han, et al., miRNA-103a-3p promotes human gastric cancer cell proliferation by targeting and suppressing ATF7 in vitro, Mol. Cells 41 (2018) 390–400.
[12] G. Isani, M. Bertocchi, G. Andreani, G. Farruggia, C. Cappadone, R. Salaroli, et al., Cytotoxic Effects of Artemisia Annua L. And Pure Artemisinin on the D-17 Canine Osteosarcoma Cell Line. Oxidative Medicine and Cellular Longevity vol. 2019, (2019), p. 1615758.
[13] R. Kang, G. Kroemer, D. Tang, The tumor suppressor protein p53 and the ferroptosis network, Free Radical Biol. Med. 133 (2019) 162–168.
[14] P. Karimi, F. Islami, S. Anandasabapathy, N.D. Freedman, F. Kamangar, Gastric cancer: descriptive epidemiology, risk factors, screening, and prevention. Cancer epidemiology, biomarkers & prevention : a publication of the American Association for Cancer Research, cosponsored by the, Am. Soc. Prev. Oncol. 23 (2014) 700–713.
[15] H.J. Li, X. Li, H. Pang, J.J. Pan, X.J. Xie, W. Chen, Long non-coding RNA UCA1 promotes glutamine metabolism by targeting miR-16 in human bladder cancer, Jpn. J. Clin. Oncol. 45 (2015) 1055–1063.
[16] J.J. Li, Y.Y. Yan, H.M. Sun, Y. Liu, C.Y. Su, H.B. Chen, et al., Anti-cancer effects of pristimerin and the mechanisms: a critical review, Front. Pharmacol. 10 (2019) 746.
[17] Q. Li, Q.Q. Li, J.N. Jia, Q.Y. Sun, H.H. Zhou, W.L. Jin, et al., Baicalein exerts neuroprotective effects in FeCl3-induced posttraumatic epileptic seizures via suppressing ferroptosis, Front. Pharmacol. 10 (2019) 638.
[18] W. Li, F. Li, Y. Zhu, D. Song, Physcion 8-O-beta-glucopyranosideregulates cell cycle, apoptosis, and invasion in glioblastoma cells through modulating Skp2, Biomed. Pharmacother. 95 (2017) 1129–1138.
[19] M. Luo, L. Wu, K. Zhang, H. Wang, T. Zhang, L. Gutierrez, et al., miR-137 regulates ferroptosis by targeting glutamine transporter SLC1A5 in melanoma, Cell Death Differ. 25 (2018) 1457–1472.
[20] E. Majewska, R. Rola, M. Barczewska, J. Marquez, J. Albrecht, M. Szeliga, Transcription factor GATA3 expression is induced by GLS2 overexpression in a glioblastoma cell line but is GLS2-independent in patient-derived glioblastoma, J. Physiol. Pharmacol. : Off. J. Pol. Physiol. Soc. 68 (2017) 209–214.
[21] G.A. Malfa, B. Tomasello, R. Acquaviva, C. Genovese, A. La Mantia, F.P. Cammarata, et al., Betula etnensis raf. (Betulaceae) extract induced HO-1 expression and ferroptosis cell death in human colon cancer cells, Int. J. Mol. Sci. 20 (11) (2019 Jun 3).
[22] J.M. Mates, J.A. Campos-Sandoval, J. de Los Santos-Jimenez, J.A. Segura, F.J. Alonso, J. Marquez, Metabolic reprogramming of cancer by chemicals that target glutaminase isoenzymes, Curr. Med. Chem. (2019).
[23] M. Munksgaard Thoren, M. Vaapil, J. Staaf, M. Planck, M.E. Johansson, S. Mohlin, et al., Myc-induced glutaminolysis bypasses HIF-driven glycolysis in hypoxic small cell lung carcinoma cells, Oncotarget 8 (2017) 48983–48995.
[24] K. Piletic, T. Kunej, MicroRNA epigenetic signatures in human disease, Arch. Toxicol. 90 (2016) 2405–2419.
[25] N. Shomali, B. Mansoori, A. Mohammadi, N. Shirafkan, M. Ghasabi, B. Baradaran, MiR-146a functions as a small silent player in gastric cancer, Biomed. Pharmacother. 96 (2017) 238–245.
[26] X. Sui, R. Zhang, S. Liu, T. Duan, L. Zhai, M. Zhang, et al., RSL3 drives ferroptosis through GPX4 inactivation and ROS production in colorectal cancer, Front. Pharmacol. 9 (2018) 1371.
[27] F. Tao, Y. Zhang, Z. Zhang, The role of herbal bioactive components in mitochondria function and cancer therapy, Evid. Based Complement Altern. Med. : eCAM 2019 (2019) 3868354.
[28] V.H. Villar, R.V. Duran, Glutamoptosis: a new cell death mechanism inhibited by autophagy during nutritional imbalance, Autophagy 13 (2017) 1078–1079.
[29] M. Wang, C. Mao, L. Ouyang, Y. Liu, W. Lai, N. Liu, et al., Long noncoding RNA LINC00336 inhibits ferroptosis in lung cancer by functioning as a competing endogenous RNA, Cell Death Differ. 26 (11) (2019 Nov) 2329–2343.
[30] Q. Wang, Y. Jiang, R. Guo, R. Lv, T. Liu, H. Wei, et al., Physcion 8-O-beta-glucopyranoside suppresses tumor growth of Hepatocellular carcinoma by downregulating PIM1, Biomed. Pharmacother. 92 (2017) 451–458.
[31] Q. Wang, Y. Wang, Y. Xing, Y. Yan, P. Guo, J. Zhuang, et al., Physcion 8-O-beta-glucopyranoside induces apoptosis, suppresses invasion and inhibits epithelial to mesenchymal transition of hepatocellular carcinoma HepG2 cells, Biomed. Pharmacother. 83 (2016) 372–380.
[32] Q. Wang, Y. Yan, J. Zhang, P. Guo, Y. Xing, Y. Wang, et al., Physcion 8-O-beta-glucopyranoside inhibits clear-cell renal cell carcinoma bydownregulating hexokinase II and inhibiting glycolysis, Biomed. Pharmacother. 104 (2018) 28–35.
[33] S. Wang, J. Luo, Z. Zhang, D. Dong, Y. Shen, Y. Fang, et al., Iron and magnetic: new research direction of the ferroptosis-based cancer therapy, Am. J. Cancer Res. 8 (2018) 1933–1946.
[34] Z. Wang, H. Yang, EMMPRIN, SP1 and microRNA-27a mediate physcion 8-O-beta-glucopyranoside-induced apoptosis in osteosarcoma cells, Am. J. Cancer Res. 6 (2016) 1331–1344.
[35] F.J. Xiao, D. Zhang, Y. Wu, Q.H. Jia, L. Zhang, Y.X. Li, et al., miRNA-17-92 protects endothelial cells from erastin-induced ferroptosis through targeting the A20-ACSL4 axis, Biochem. Biophys. Res. Commun. 515 (2019) 448–454.
[36] Li Xun, Y. Liu, S. Chu, S. Yang, Y. Peng, S. Ren, et al., Physcion and physcion 8-O-beta-glucopyranoside: a review of their pharmacology, toxicities and pharmacokinetics, Chem. Biol. Interact. 310 (2019) 108722.
[37] H. Yu, C. Yang, L. Jian, S. Guo, R. Chen, K. Li, et al., Sulfasalazineinduced ferroptosis in breast cancer cells is reduced by the inhibitory effect of estrogen receptor on the transferrin receptor, Oncol. Rep. 42 (2) (2019 Aug) 826–838.
[38] D. Zhang, Y. Han, L. Xu, Upregulation of miR-124 by physcion 8-O-beta-glucopyranoside inhibits proliferation and invasion of malignant melanoma cells via repressing RLIP76, Biomed. Pharmacother. 84 (2016) 166–176.
[39] H. Zhang, M. Zhu, X. Shan, X. Zhou, T. Wang, J. Zhang, et al., A panel of seven-miRNA signature in plasma as potential biomarker for colorectal cancer diagnosis, Gene 687 (2019) 246–254.
[40] K. Zhang, L. Wu, P. Zhang, M. Luo, J. Du, T. Gao, et al., miR-9 regulates ferroptosis by targeting glutamic-oxaloacetic transaminase GOT1 in melanoma, Mol. Carcinog. 57 (2018) 1566–1576.
[41] X. Zhang, L. Du, Y. Qiao, X. Zhang, W. Zheng, Q. Wu, et al., Ferroptosis is governed by differential regulation of transcription in liver cancer, Redox Biol 24 (2019) 101211.